

Altered Expression Pattern of Polycystin-2 in Acute and Chronic Renal Tubular Diseases

NICHOLAS OBERMÜLLER,^{*†} YIQIANG CAI,[‡] BETTINA KRÄNZLIN,^{*}
R. BRENT THOMSON,[‡] NORBERT GRETZ,^{*} WILHELM KRIZ,^{||}
STEFAN SOMLO,^{‡§} and RALPH WITZGALL^{||}

^{*}Medical Research Center, Klinikum Mannheim, University of Heidelberg, Mannheim, Germany; [†]Section of Nephrology, Department of Internal Medicine IV, University of Frankfurt, Frankfurt, Germany; [‡]Department of Medicine, Section of Nephrology, and [§]Department of Genetics, Yale University School of Medicine, New Haven, Connecticut; and ^{||}Institute for Anatomy and Cell Biology I, University of Heidelberg, Heidelberg, Germany.

Abstract. Polycystin-2 represents one of so far two proteins found to be mutated in patients with autosomal-dominant polycystic kidney disease. Evidence obtained from experiments carried out in cell lines and with native kidney tissue strongly suggests that polycystin-2 is located in the endoplasmic reticulum. In the kidney, polycystin-2 is highly expressed in cells of the distal and connecting tubules, where it is located in the basal compartment. It is not known whether the expression of polycystin-2 in the kidney changes or whether it can be manipulated under certain instances. Therefore, the distribution of polycystin-2 under conditions leading to acute and chronic renal failure was analyzed. During ischemic acute renal failure, which affects primarily the S3 segment of the proximal tubule, a pronounced upregulation of polycystin-2 and a predominantly combined homogeneous and punctate cytoplasmic distribution in damaged cells was observed. After thallium-induced acute injury to thick ascending limb cells, polycystin-2

staining assumed a chicken wire–like pattern in damaged cells. In the (*cy/+*) rat, a model for autosomal-dominant polycystic kidney disease in which cysts originate predominantly from the proximal tubule, polycystin-2 immunoreactivity was lost in some distal tubules. In kidneys from (*pcy/pcy*) mice, a model for autosomal-recessive polycystic kidney disease in which cyst formation primarily affects distal tubules and collecting ducts, a minor portion of cyst-lining cells cease to express polycystin-2, whereas in the remaining cells, polycystin-2 is retained in their basal compartment. Data show that the expression and cellular distribution of polycystin-2 in different kinds of renal injuries depends on the type of damage and on the nephron-specific response to the injury. After ischemia, polycystin-2 may be upregulated by the injured cells to protect themselves. It is unlikely that polycystin-2 plays a role in cyst formation in the (*cy/+*) rat and in the (*pcy/pcy*) mouse.

Autosomal-dominant polycystic kidney disease (ADPKD) has an approximate prevalence of 1:1000 (1,2) and accounts for 8 to 10% of all cases of end-stage renal disease in Western countries (3–7). Although this hereditary disorder affects primarily the kidney, additional extrarenal manifestations emphasize the systemic character of the disease. As a result of major efforts over the last few years, the two most frequently mutated genes in ADPKD, *PKD1* (8) and *PKD2* (9), have been identified. Mutations in the *PKD1* gene are responsible for approximately 85% of all ADPKD cases, whereas the majority of the remaining patients experience mutations in the *PKD2* gene (10–13). A very small group of ADPKD patients possibly

carry mutations in genes that are as yet unidentified (14–17). Although there is a high degree of similarity with respect to the spectrum of renal and extrarenal disease manifestations between the two forms, patients with *PKD2* mutations have a milder phenotype and a delayed onset compared with patients with mutations in the *PKD1* gene (13,18–22). Moreover, the organ-specific phenotypes of *Pkd1* (23–25) and *Pkd2* (26,27) knockout mice show striking similarities. Current data support the view that the loss of function of *PKD1* and *PKD2* is the responsible mechanism for cyst development in patients with ADPKD (28), but the definite roles of both proteins in cystogenesis is still unclear.

The *PKD2* gene, located on chromosome 4, spans approximately 68 kbp and encodes a 5.4-kb transcript. The resulting protein product, polycystin-2, is a 968–amino acid protein with a predicted size of 110 kD. Polycystin-2 is an integral membrane protein with six putative transmembrane spanning domains and intracellular NH₂- and COOH-termini. It shows sequence similarities to voltage-activated calcium channels, to calcium channels of the transient receptor potential (Trp) family, and also to polycystin-1 (9). A number of studies have examined the distribution of polycystin-2 by immunocytochemistry

Received October 1, 2002. Accepted March 27, 2002.

Correspondence to Dr. Ralph Witzgall, Institute for Anatomy and Cell Biology I, University of Heidelberg, Im Neuenheimer Feld 307, 69120 Heidelberg, Germany. Phone: +49-6221-548686; Fax: +49-6221-544951; E-mail: ralph.witzgall@urz.uni-heidelberg.de

1046-6673/1307-1855

Journal of the American Society of Nephrology
Copyright © 2002 by the American Society of Nephrology

DOI: 10.1097/01.ASN.0000018402.33620.C7

in rodent as well as in human tissues, and both during development and in differentiated organs (29–32). There is now strong evidence that in the kidneys of several species, polycystin-2 is strongly expressed in the basal compartment of the entire distal tubule and of the collecting duct. In many other organs, however, polycystin-2 immunoreactivity shows a more punctate cytoplasmic expression pattern (30). Moreover, *in vitro* and *in vivo* studies have demonstrated that polycystin-2 is located in the endoplasmic reticulum (33–35) and at the same time is linked to the actin cytoskeleton (34), a fact that could explain the formation of cysts in the kidney and in other organs.

The possible involvement of polycystin-2 in cell-matrix complexes raises the question whether the expression and/or subcellular distribution of this protein is affected by specific insults. A characterization of polycystin-2 during such events could offer new insights for its role in polycystic kidney disease (PKD) and other disease states, but so far, no investigations have been performed to address this issue. Therefore, the immunohistochemical expression pattern of the polycystin-2 protein was examined in two acute forms of tubular insults in the rat kidney: ischemic acute renal failure and thallium-induced nephrotoxicity. In addition the expression of polycystin-2 was evaluated in two rodent models for PKD, the (*cy/+*) rat and the (*pcy/pcy*) mouse, which represent chronic types of tubulointerstitial disease.

Materials and Methods

Animals

Animals were kept under standard laboratory conditions in an animal care facility in Mannheim, Germany. All animals were allowed free access to tap water and chow containing 19% protein. Male adult Sprague-Dawley rats (70 to 100 d old), male (*cy/+*) rats (4 to 6 mo old) as well as male (*pcy/pcy*) mice (5 and 13 wk old) were chosen for the different experimental procedures. The (*cy/+*) rats are originally derived from the Han:SPRD rat strain (36–38). This colony has now been inbred for more than 20 generations in Mannheim and has been registered as follows: polycystic kidney disease, Mannheim (PKD/Mhm, Inbred Strains of Rats, <http://www.informatics.jax.org/external/festing/rat/docs/PKD.shtml>). All experiments were performed in accordance with federal and local laws, as well as institutional regulations. Male (*pcy/pcy*) mutant mice used in this study were a gift from Dr. J. Grantham, Kansas City, KS, and have been characterized elsewhere (39,40).

Induction of Bilateral Ischemic Acute Renal Failure

This procedure was performed as previously described (41). Sprague-Dawley rats were deeply anesthetized by an intramuscular injection of ketamine (100 mg/kg) and xylazine (5 mg/kg). After a midline incision was made, the left and right renal pedicles were located. Next, 100 IU of heparin (in 1 ml of 0.9% NaCl) were injected into the tail vein, and both renal arteries were occluded with a microaneurysm clamp for a period of 45 min. To balance the fluid loss caused by evaporation, 1 ml of 0.9% NaCl was administered to the peritoneal cavity. Sham-operated animals were treated similarly to the ischemic animals, with the exception that the renal pedicles were not clamped; instead, both renal hila were softly touched. At the end of the ischemic period, clamps were removed, and the successful and homogeneous reperfusion of the kidneys was documented by inspec-

tion before the abdominal incisions were sutured. Animals then received an intramuscular injection of 0.02 mg buprenorphine/kg as analgesia.

After defined periods of reperfusion (0, 4, 12, and 18 h as well as 1, 2, and 16 d after ischemia, $n = 2$ to 4) the animals were subjected to perfusion fixation. Blood samples were taken from the animals 1 d before and 24 h after ischemia and at the end of the different reperfusion times to assess the transient peaks of serum creatinine and urea levels in the postischemic animals. In postischemic rats, serum creatinine and urea levels returned to baseline values 7 d after the ischemic insult.

Thallium-Induced Nephrotoxic Damage in the Thick Ascending Limb

These experiments were performed with minor modifications as described earlier (42). Thallium sulfate (Fluka Chemie, Taufkirchen, Germany) was dissolved in a 0.9% NaCl solution at a concentration of 0.4 mg Tl_2SO_4 /ml. Rats received intraperitoneal injections of 20 mg Tl_2SO_4 /kg. The administration of this dose has been shown to result in severe morphologic changes in thick ascending limb cells (42). Control rats received corresponding saline volumes without thallium sulfate. Thallium- or vehicle-treated rats were housed in pairs in cages. No evident abnormalities in the behavior of the rats due to potential systemic effects of Tl_2SO_4 were noticed. Only 8 d after thallium sulfate administration, rats showed restricted areas of hair loss in their neck regions.

At different time points after the administration of thallium sulfate (days 1, 2, 3, 4, 5, 6, and 8; $n = 3$ of each time point), rats were subjected to perfusion fixation. For the biochemical analysis, kidneys were removed 2 d after the injection of thallium and homogenized as described before (33). Approximately 350 μ g of total protein was digested with endoglycosidase H (New England Biolabs, Beverly, MA) and then analyzed by Western blot test with the polyclonal anti-polycystin-2 antibody YCC2 (diluted 1:5000) (33).

Perfusion-Fixation

Male Sprague-Dawley rats as well as male (*cy/+*) rats and (*pcy/pcy*) mice were anesthetized by an intramuscular injection of ketamine (100 mg/kg) and xylazine (5 mg/kg). Animals were perfused retrogradely through the infrarenal abdominal aorta. The perfusion was conducted with 4% freshly depolymerized paraformaldehyde in phosphate-buffered saline (PBS), pH 7.4, for 3 min at a pressure level of 180 mmHg. Kidneys were removed, cut into slices, and immersed in the same fixative overnight before being embedded in paraffin for subsequent histologic examination by immunohistochemistry and hematoxylin and eosin (HE) staining. In addition, thin kidney slices from rats treated with thallium sulfate were immersed in 2% glutaraldehyde/2% paraformaldehyde in PBS, pH 7.4, overnight for subsequent ultrastructural analysis.

High-Resolution Light Microscopy and Transmission Electron Microscopy

Kidney samples were incubated in 1% osmium tetroxide and embedded in Epon-812. One-micron-thick sections were cut on an ultramicrotome, stained with azure II/methylene blue, and examined by light microscopy. Ultrathin sections were cut with a diamond knife on an ultramicrotome and placed on Formvar-coated copper grids. The sections were first stained in 5% uranyl acetate for 15 min and subsequently for 2 min in Reynold lead citrate before being viewed under a Philips EM301 electron microscope.

Immunohistochemistry

Sections (3 to 4 μm thick) from which the paraffin had been removed were washed in PBS and incubated with blocking solution (2% bovine serum albumin in PBS) at room temperature in a humid chamber. The sections were then incubated with one of the following antibodies: the rabbit polyclonal anti-polycystin-2 antibody YCC2, directed against amino acids 687 to 962 of human polycystin-2 (diluted 1:400) (26); a rabbit polyclonal antibody against the α_1 subunit of Na^+/K^+ -ATPase (diluted 1:200; Upstate Biotechnology, Lake Placid, NY); a polyclonal antibody against E-cadherin (diluted 1:200; Sigma, Deisenhofen, Germany).

For immunohistochemistry with E-cadherin, sections were subjected to microwave treatment before the normal immunostaining protocol. In brief, after washing in PBS, sections were placed in 10 mM citric acid pH 6.0 and heated in a microwave oven at 600 W for 5×5 min. Thereafter, slides were allowed to cool to room temperature before the blocking step commenced. The primary antibodies were applied for 2 h at room temperature and subsequently overnight at 4°C. Thereafter, slides were rinsed twice for 10 min in PBS and incubated with a Cy3-coupled secondary antibody (Dianova, Hamburg, Germany) for 1 h at room temperature. After washing in PBS, sections were mounted in PBS-buffered glycerol. For a better morphologic analysis of the immunohistochemical results, some sections were subjected to HE staining after documentation of the immunofluorescence results.

Control incubations on adjacent sections were performed with normal rabbit serum instead of the primary antibody. To further control for the specificity of the anti-polycystin-2 antibody YCC2, the antibody was preabsorbed for 30 min with either glutathione *S*-transferase (2 ng/ μl) or the glutathione *S*-transferase-polycystin-2 fusion protein (4 ng/ μl) used to generate the polyclonal antibody (these concentrations correspond to approximately equimolar amounts of both proteins). After the preabsorption step, the antibody was applied to the sections; otherwise, the staining protocol was followed as described above.

Processing of Images

Black-and-white photographs from HE- and azure II/methylene blue-stained sections as well as from immunofluorescence-labeled sections were scanned with a Nikon Coolscan LS-2000 via Silverfast 4.1 software (LaserSoft, Kiel, Germany). Transmission electron micrographs were scanned with a Linotype Saphir ultrascanner by Linocolor 5.1 software. All files were thereafter processed with Photoshop 5.5 (Adobe Systems, San Jose, CA).

Results

Under normal conditions, polycystin-2 expression in the rat kidney is strong in distal tubules but weak or undetectable in proximal tubules (30). To investigate the expression of polycystin-2 under conditions of acute renal failure, the injurious effect of ischemia, which mainly affects proximal tubular cells, and the toxic effect of thallium sulfate on thick ascending limb cells were analyzed.

Immunohistochemical Distribution of Polycystin-2 in the Postischemic Kidney

Four hours after the ischemic insult, the distribution of polycystin-2 did not vary from that in sham-operated animals (Figure 1i)—that is, a strong basal expression of the protein in distal tubules of the adult rat kidney was observed as described

recently (30). At 12, 18, and 24 h after ischemia, a strong basal-to-basolateral signal was still detected in cells of the distal tubule; however, an increasingly prominent expression of the protein could now be found in tubular cells of the S3 segment in the outer stripe, the major site of injury (43). This was evident in profiles, which showed the characteristic signs of acute tubular damage—for example, rounding of cells, cells detaching from the basement membrane, and accumulation of cellular debris in the lumen (Figure 1a and b). Polycystin-2 immunoreactivity was not found uniformly in damaged cells but rather showed distinct patterns. In some proximal tubular cells, which still appeared to line the basement membrane, a strong basal-to-basolateral expression could be observed (Figure 1c), which resembled the distribution known from regular distal tubular cells. Cells already floating in the tubular lumen sometimes still exhibited a polarized staining pattern, but in numerous detached cells, a pronounced punctate distribution of polycystin-2 was noted (Figure 1c). Apart from the increased expression of polycystin-2 in postischemic proximal tubular cells of the S3 segment, strong immunoreactivity was also observed in proximal tubular cells of the S1 segment (Figure 1g and h). This observation was already found on kidney sections 12 h after the ischemic insult, but was a much more frequent finding at 18 and 24 h after ischemia.

Two days after the ischemic insult, the polycystin-2 protein was still present in detached tubular cells floating in the luminal space of proximal tubules in the outer stripe (Figure 1d and e). The immunohistochemical staining pattern demonstrated a combined homogeneous and punctate cytoplasmic distribution of polycystin-2 (Figure 1f). In contrast, distal tubular profiles showed a very faint or even absent immunohistochemical signal for polycystin-2 at this time point. At 16 d after ischemia, the characteristic intrarenal distribution of polycystin-2 with a basal staining pattern in distal tubules could be observed at a strength comparable to sham-operated or normal adult animals.

Omission of the polyclonal anti-polycystin-2 antibody, or preabsorbing it with the recombinant peptide used for immunizing the rabbits abolished the staining in the damaged S3 segments (data not shown), thus corroborating the immunohistochemical results.

Immunohistochemical Distribution of Polycystin-2 after Thallium-Induced Injury

Thallium is similar in its physicochemical characteristics to potassium, and thus it substitutes for potassium in a variety of physiologic reactions. Moreover, its affinity for the Na^+/K^+ -ATPase is 10 times higher than that of potassium. Previous studies have shown that treatment with thallium leads to distinct pathologic changes—in particular, in the thick ascending limb—approximately 2 d after administration of the chemical (42).

Analysis of semithin sections obtained from kidneys 2 d after thallium administration showed that almost all thick ascending limb profiles of the inner stripe were swollen and contained vacuoles (Figure 2a and b). The typical architecture of the basolateral interdigitations was drastically reduced or

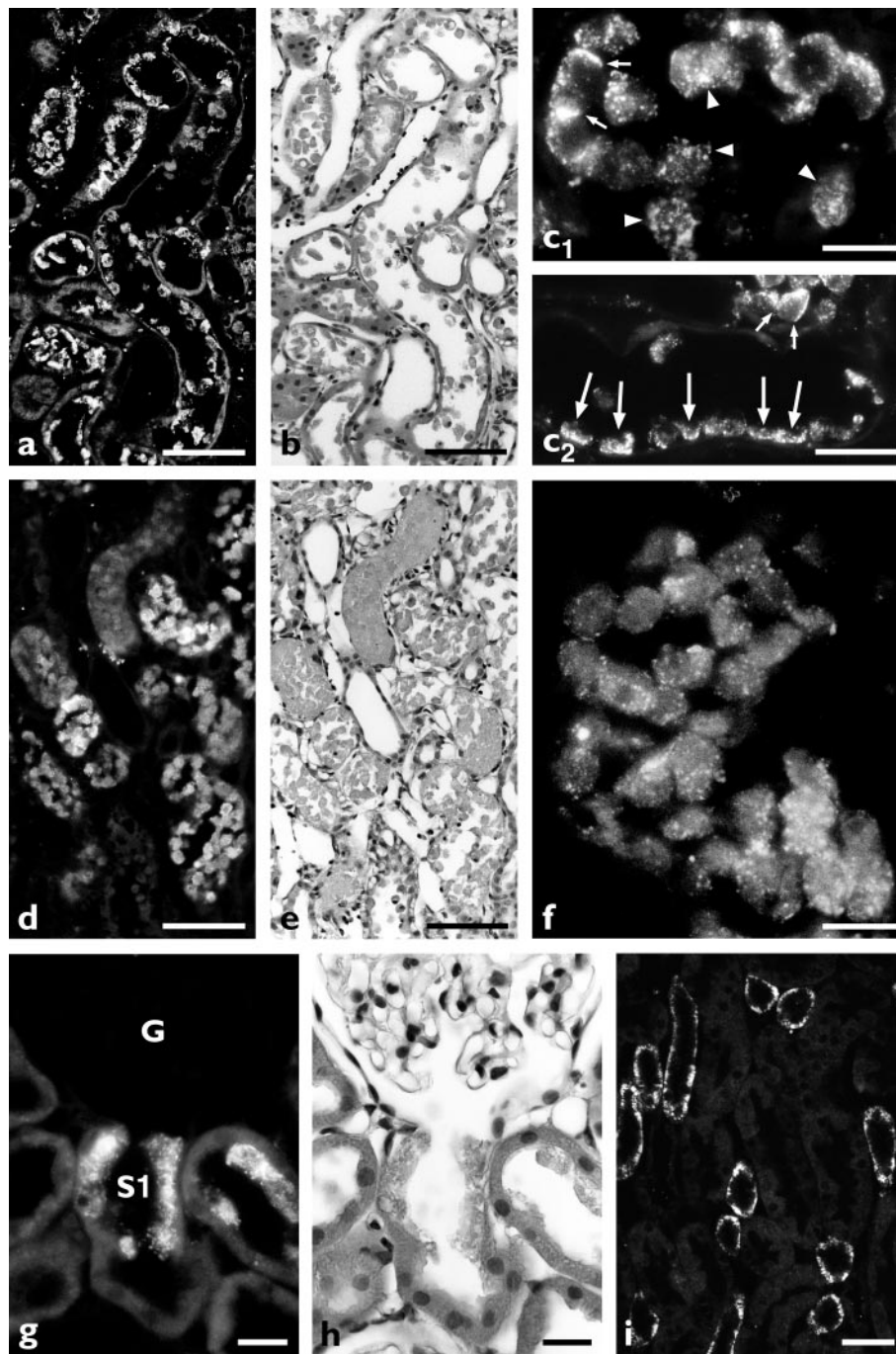


Figure 1. Expression of polycystin-2 after ischemic injury. (a to c) Twenty-four hours after bilateral clamping of the renal pedicles for 45 min. An overview of the outer stripe stained with the anti-polycystin-2 antibody YCC2 demonstrates a strong expression of polycystin-2 in tubular cells of the S3 segment, which are in the process of lifting off the basement membrane (immunofluorescence in a, hematoxylin and eosin [HE] staining in b). At higher magnification, different distributions of polycystin-2 can be seen. Some cells still showed a lateral (small arrows) or basal (large arrows) staining with the anti-polycystin-2 antibody, whereas in many cells, a combined homogeneous and punctate distribution of polycystin-2 in the cytoplasm was observed (arrowheads) (c₁, c₂). (d to f) Forty-eight hours after bilateral clamping of the renal pedicles for 45 min. The luminal debris originating from detached tubular cells stains brightly with the anti-polycystin-2 antibody (immunofluorescence in d, HE staining in e). A higher magnification demonstrates the combined homogeneous and punctate distribution in the cytoplasm of all those cells (f). (g, h) Eighteen hours after the ischemic insult. These panels demonstrate the induction of polycystin-2 in the initial portion of the S1 segment of the proximal tubule (g). Counterstaining with HE shows the foamy appearance of the cells expressing polycystin-2, indicating that those cells are injured (h). (i) Forty-eight hours after a sham operation. Polycystin-2 is located in the basal compartment of distal tubules traversing the outer stripe. G, glomerulus; S1, S1 segment of the proximal tubule. Bars, 100 μ m (a, b, d, e), 20 μ m (c₁, f to h), 40 μ m (c₂, i).

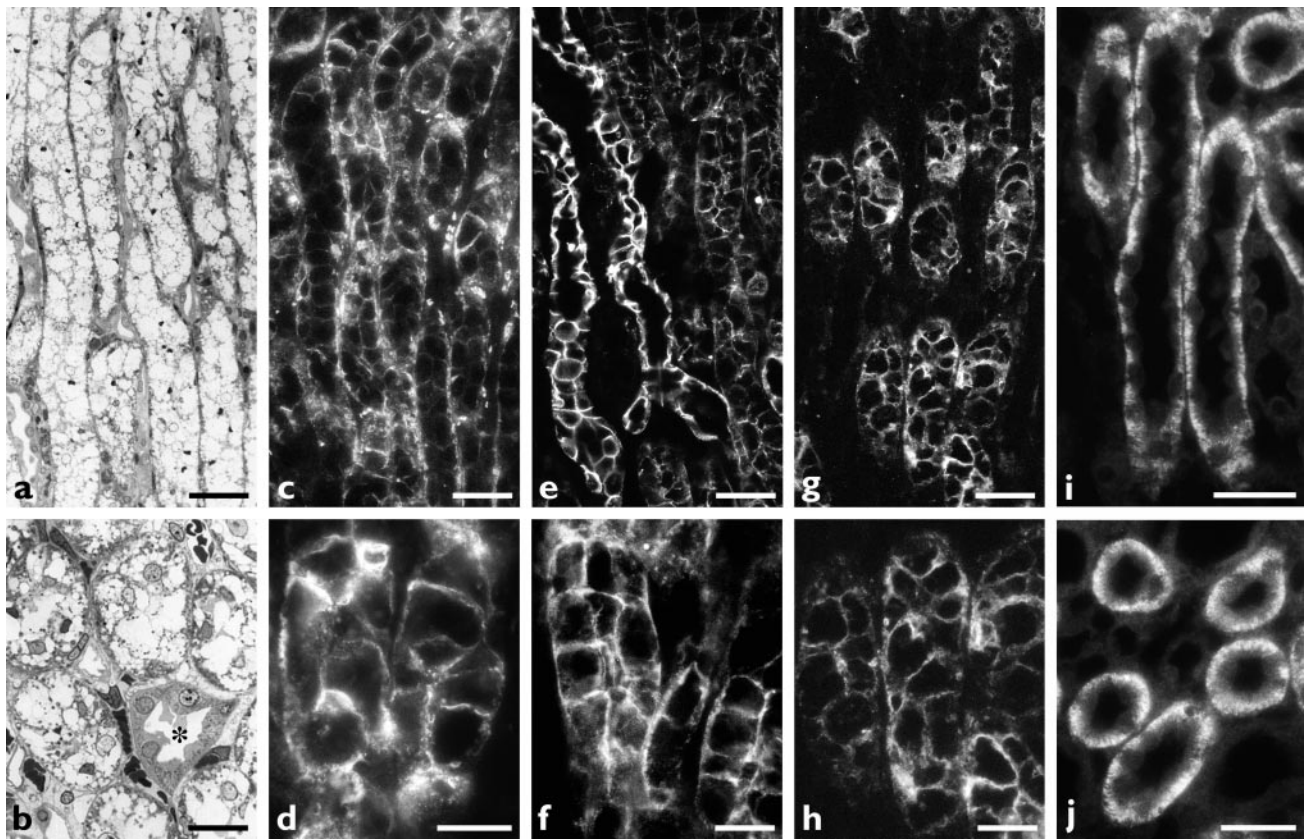


Figure 2. Expression of polycystin-2, E-cadherin, and Na^+/K^+ -ATPase 48 h after injection of thallium. (a, b) The administration of thallium results in the vacuolar appearance of thick ascending limb cells in the inner stripe (overview of a semithin section in a, higher magnification in b), whereas a collecting duct (asterisk) is not damaged. (c, d) Staining with the anti-polycystin-2 antibody demonstrates the chicken wire-like distribution of the protein. (e to h) Further characterization of the injured thick ascending limb cells revealed that E-cadherin (e, f) and Na^+/K^+ -ATPase (g, h) are also located on the cell periphery. (i, j) Longitudinal profiles and cross sections of thick ascending limbs in the inner stripe 2 d after the intraperitoneal injection of a 0.9% NaCl solution. Immunofluorescence staining demonstrates the location of polycystin-2 in the basal compartment of these cells. Bars, 50 μm (a, c, e, g, i, j), 20 μm (b, d, f, h).

even absent in many cells. In the vast majority, despite the drastic morphologic changes, the thick ascending limb cells still seemed to adhere to the basement membrane and to each other. Collecting duct profiles traversing the inner stripe did not show marked morphologic changes (Figure 2b). Already 3 d after thallium administration, most of the thick ascending limb profiles exhibited an almost normal cellular structure. In many cells, the prominent vacuoles had disappeared, and the typical basolateral cell architecture had been reestablished. In some areas, however—for example, at the transition to the inner medulla—thick ascending limb profiles with still-swollen cells or a regenerating thin epithelial cell layer were still observed (data not shown).

The immunohistochemical analysis of polycystin-2 expression 2 d after the administration of thallium showed a pronounced staining at the cell periphery of numerous thick ascending limb cells in the inner stripe (Figure 2c and d), which is in stark contrast to its normal basal distribution (Figure 2i and j). To learn more about the intracellular distribution of polycystin-2, serial sections of the inner stripe were stained with antibodies against the Na^+/K^+ -ATPase and E-cadherin, two proteins located in the basolateral plasma membrane.

Figure 2 shows that both proteins are expressed in the thick ascending limb cells in a pattern resembling that of polycystin-2 (Figure 2e to h).

For a more comprehensive analysis of the immunohistochemical results, the ultrastructure of thick ascending limb cells 2 d after thallium-induced injury is shown in Figure 3. Apart from a rarefied basolateral plasma membrane, an intracellular membrane could often be identified immediately beneath the plasma membrane. The latter membrane lined large vesicular structures, which probably correspond to the endoplasmic reticulum and which could explain the immunohistochemical staining pattern with the anti-polycystin-2 antibody (Figure 3, a and b). To provide further evidence for the assumption that polycystin-2 still resided in the endoplasmic reticulum, total kidney extracts were subjected to a treatment with endoglycosidase H (endo H). Endo H can only remove sugars from glycoproteins that have not progressed beyond the *cis* compartment of the Golgi apparatus. As shown recently, endogenous polycystin-2 from native kidneys is sensitive to a digest with endo H (35), consistent with its location in the endoplasmic reticulum. Polycystin-2 isolated from kidneys 2 d after the administration of thallium showed the same mobility

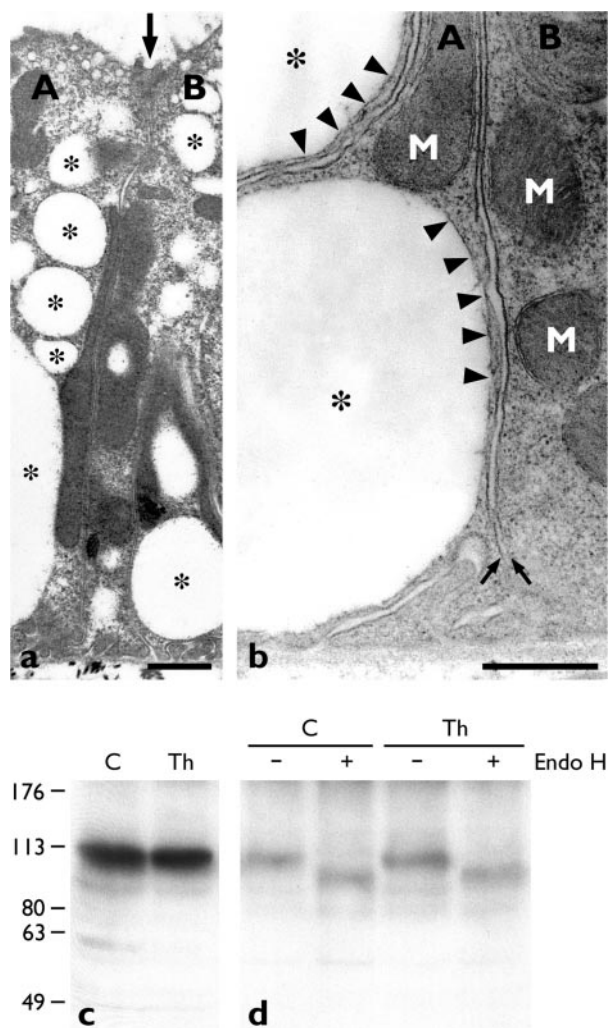


Figure 3. Evidence for the location of polycystin-2 in the endoplasmic reticulum after thallium-induced damage. (a, b) Ultrastructural changes in thick ascending limb cells after administration of thallium. A low-power magnification demonstrates many vacuoles (asterisks) in two adjacent cells (arrow indicates the border between cells A and B) (a). At a higher magnification, it is possible to note that those vacuoles (asterisks) are lined by a membrane (arrowheads) such that this membrane comes to lie immediately below the plasma membranes (arrows) of cells A and B (b). (c, d) Western blot analysis of polycystin-2. Polycystin-2 from kidneys of both saline- and thallium-treated rats shows the same mobility (c) and is sensitive to treatment with endoglycosidase H (d). The numbers on the left represent the M_r (kD). M, mitochondria; C, rats injected with a 0.9% NaCl solution; Th, rats injected with thallium. Bars, 1 μm (a), 0.5 μm (b).

as that from kidneys of saline-injected rats (Figure 3c); furthermore, it was fully sensitive to endo H (Figure 3d). These findings therefore argue that polycystin-2 is still located in the endoplasmic reticulum, even after thallium-induced injury.

Distribution of Polycystin-2 in (cy/+) Rat and (pcy/ pcy) Mouse Kidneys

Although a number of spontaneous rodent models for PKD have been described, none of them arise from mutations in

Pkd1 and *Pkd2*. It is possible, however, that the intracellular location and the activity of polycystin-1 and -2 are influenced by the proteins mutated in those animal models, and therefore the expression pattern of polycystin-2 in such models may provide valuable information. For our analysis, we chose the (cy/+) rat, a model for autosomal-dominant PKD, and the (pcy/pcy) mouse, a model for autosomal-recessive polycystic kidney disease.

In the (cy/+) rat, cysts originate almost exclusively from proximal tubules (36–38). Neither epithelial cells of normal nor of cystic proximal tubules were stained by the anti-polycystin-2 antibody. Comparable to the situation in normal adult rat kidneys, the immunohistochemical analysis of polycystin-2 showed a strong basal staining in distal tubules of 4-mo-old (cy/+) rats. Occasionally occurring dilated distal tubules in the cortex also exhibited the typical basal expression of the protein. Interestingly, some moderately dilated thick ascending limb profiles in the inner stripe showed a very intense signal when compared with the fluorescence intensity of thick ascending limb profiles of wild-type or normal kidneys. In addition, in some thick ascending limb profiles located in the inner stripe, polycystin-2 immunoreactivity had disappeared in a mosaic pattern (Figure 4a). Serial sections labeled with an anti- Na^+/K^+ -ATPase antibody and with the anti-polycystin-2

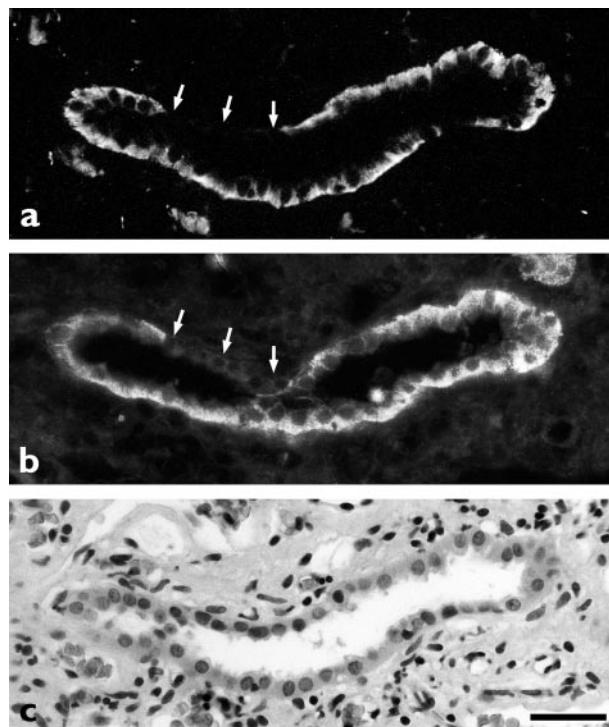


Figure 4. Expression of polycystin-2 and Na^+/K^+ -ATPase in a distal tubule of the (cy/+) rat kidney. (a) Whereas most cells of this distal tubule show the typical basal distribution of polycystin-2, some cells have ceased to express polycystin-2 (arrows). (b) Neighboring section stained with an antibody against Na^+/K^+ -ATPase, demonstrating that the same cells, which do not express polycystin-2, have also drastically downregulated the expression of Na^+/K^+ -ATPase. (c) Hematoxylin and eosin staining of the section shown in (a). Bar, 40 μm .

antibody showed that those epithelial cells, which did not express polycystin-2 any longer, also had lost the ability to express Na^+/K^+ -ATPase (Figure 4b).

Renal cysts in (*pcy/pcy*) mice develop predominantly from distal tubules and collecting ducts (40). In kidney sections of 13-wk-old (*pcy/pcy*) mice, the typical basal distribution of polycystin-2 expression could be detected in nondilated distal tubules (Figure 5a). At this age, numerous cysts were found throughout the kidney. Some cystic profiles in the cortex and in the medulla, especially larger cysts with flattened epithelial cells, were completely devoid of an immunohistochemical signal for polycystin-2 (Figure 5b). Other cysts demonstrated the typical basal distribution of polycystin-2 in one part of the cyst-lining epithelium, but no polycystin-2 immunoreactivity in other portions of the cyst (Figure 5c and d). The findings in 5-wk-old (*pcy/pcy*) mouse kidneys were similar, although cysts were found less frequently (data not shown).

Discussion

These data here describe the expression pattern of polycystin-2 in acute and chronic forms of renal failure. Because the exact role of polycystin-2 in normal tubular cells and during cystogenesis has not been determined yet, the examination of its expression pattern in various pathologic situations may help to shed some light on its function.

In postischemic kidneys, we demonstrated an increased expression of polycystin-2, mainly in cells originating from the S3 segment of the proximal tubule. This was most evident between 12 and 48 h after ischemia, when maximal damage develops in the outer stripe (43,44). At early time points, injured cells of the S3 segment showed an increased basal to basolateral staining pattern, which later changed to a more homogeneous and punctate cytoplasmic polycystin-2 distribution, when the cells had lost contact to the basement membrane

and were present in the tubular lumen. It can therefore be assumed that the changes in the intracellular distribution of polycystin-2 correlate with the complex cascade after acute ischemia—that is, cellular injury, detachment from the basement membrane and cell death. The distinct intracellular distribution of polycystin-2 (basal-to-basolateral *versus* homogeneous and punctate cytoplasmic) observed in proximal tubules may be due to the loss of cell polarity, the disintegration of the cytoskeleton, and the disruption of cell contacts, which are all associated with ischemia-reperfusion injury. In the setting of the postischemic kidney, the upregulation of polycystin-2 may serve to maintain crucial cell structures such as cell-cell or cell-matrix contacts, as has been proposed for this protein.

It has long been documented that the S3 segment is the portion of the proximal tubule most susceptible to ischemic injury (43). However, during our immunohistochemical analysis, we consistently noted an increased expression of polycystin-2 in the initial portion of the proximal convoluted tubule. Also at this location, tubular damage, which ultimately leads to cell detachment, was associated with the strong expression of polycystin-2, thus mimicking the situation observed in the outer stripe. These data show that proximal tubular cells from different segments (the S1 and the S3 segment) are capable of strongly expressing polycystin-2 in response to an ischemic insult. The fact that polycystin-2 expression could not be detected in the less compromised S1 and S2 segments suggests that the protein is only upregulated under conditions of severe cell damage.

Compared with the postischemic expression of polycystin-2 in proximal tubules, its expression in distal tubules was found to be reduced 48 h after ischemia. This reduced staining was not accompanied by a change in the intracellular distribution. It is well known that distal tubules react differently to acute renal failure than proximal tubules (45). A temporarily decreased

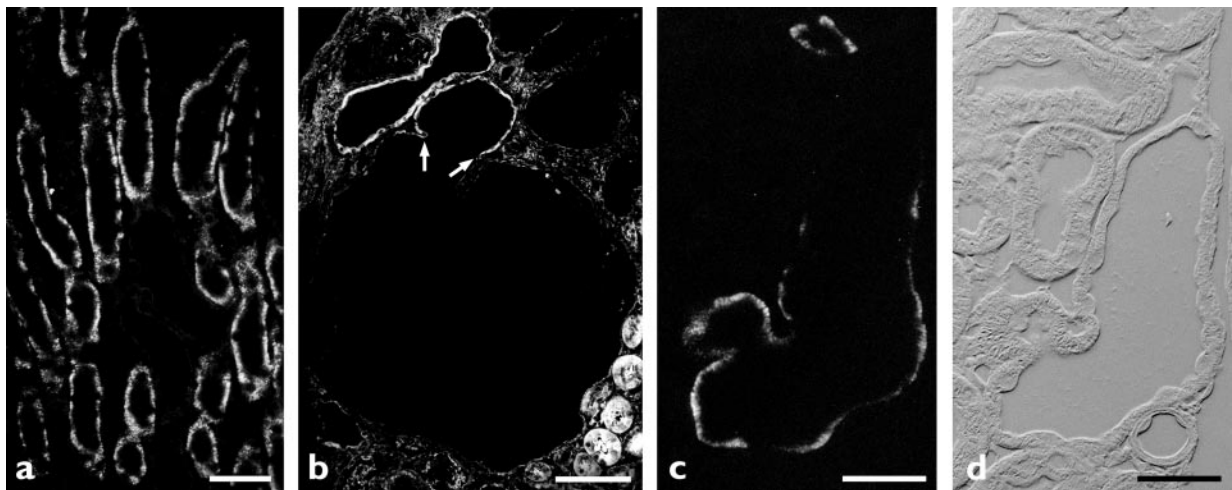


Figure 5. Expression of polycystin-2 in a 13-wk-old (*pcy/pcy*) mouse kidney. (a) Overview of the inner stripe demonstrating the strong expression of polycystin-2 in the basal compartment of noncystic thick ascending limbs. (b) At the transition from a small to a large cyst profile (arrows), the abrupt loss of polycystin-2 can be seen. (c, d) In this cyst, a mosaic distribution of polycystin-2 was detected, with some cells expressing polycystin-2 and others not. Polycystin-2 is still detected in the basal compartment of these cells (immunofluorescence in c, Nomarski optics in d). Bars, 50 μm (a), 300 μm (b), 40 μm (c, d).

expression of polycystin-2 in the distal tubule is consistent with the fact that the synthesis of other proteins such as EGF (46) and Tamm-Horsfall protein (47) is drastically reduced in this segment in response to ischemic injury.

The polycystin-2 expression pattern after thallium-induced injury to thick ascending limb cells was strikingly different from that in postischemic proximal tubules because we did not see a decreased expression, but rather a transient redistribution of polycystin-2 to the cell periphery. Thallium administration induces severe morphologic changes in thick ascending limb cells, which are reversible after a short period. A general breakdown of cellular structures and function, which may ultimately lead to cell death, does not occur. Even 2 d after thallium administration, at the time of maximal damage, tubular cells were resting on the basement membrane and cell-cell contacts were still existing as demonstrated by the chicken wire–like distribution of the cell adhesion molecule E-cadherin in injured thick ascending limb cells. The intracellular distribution of polycystin-2 in those cells resembled that of E-cadherin, but for technical reasons, it was not possible to determine whether both proteins colocalize.

So far, most experimental data support the notion that polycystin-2 is located in the endoplasmic reticulum (33–35). Although at first sight its distribution in injured thick ascending limb cells suggests that polycystin-2 has moved into the plasma membrane, the following findings suggest otherwise. We were able to detect an intracellular membrane immediately below the plasma membrane in injured cells, which probably corresponds to the membrane of the endoplasmic reticulum. Normal thick ascending limb cells are connected by lateral interdigitations, into which the endoplasmic reticulum extends (48,49). Upon thallium-induced injury, the lateral interdigitations disappear, and with them the infoldings of the endoplasmic reticulum. The large amounts of intracellular membranes have to be redistributed, and we therefore suggest that the vacuoles, which appear in the injured cells, represent the distorted endoplasmic reticulum. Although we were not able to localize polycystin-2 by immunogold electron microscopy, we could demonstrate that it was still sensitive to a treatment with endo H, thus strongly arguing that indeed it has not left the endoplasmic reticulum. Of course, polycystin-2 is also present in undamaged tubules, but a substantial portion, if not the majority of it, is found in the inner stripe (30), where most of the damage occurs after administration of thallium. For this reason, we believe that we would have detected endo H–resistant polycystin-2 had it been present, but all of it was endo H sensitive.

When compared with the situation in acute renal failure, the behavior of polycystin-2 in two forms of chronic renal failure, *i.e.*, the (*cy/+*) rat kidney and the (*pcy/pcy*) mouse kidney, was quite different. Although a strong expression of polycystin-2 was easily detectable in most distal tubules, individual distal tubular cells had apparently lost the ability to express polycystin-2 in both animal models. In the (*cy/–*) rat kidney, this was most evident in areas with advanced tubulointerstitial remodeling. The finding that those tubular cells, which did not express polycystin-2 any longer, also showed a pronounced downregulation of a typical segment-specific marker such as

Na^+/K^+ -ATPase suggests that the loss of those proteins represents a general dedifferentiation phenomenon. We emphasize, however, that some thick ascending limb profiles, which exhibited an obviously normal architecture, were stained very brightly with the anti-polycystin-2 antibody. In the (*pcy/pcy*) mouse kidney, where most cysts originate from distal tubules and collecting ducts (40), the majority of cysts still expressed polycystin-2, and no missorting of polycystin-2 could be observed in cyst-lining cells. These results argue against a role of polycystin-2 in cyst formation in either animal model.

Acknowledgments

We thank Hiltraud Hossler for performing the ultrastructural analysis and Jared Grantham for providing the CD1- (*pcy/pcy*) mice. We thank Rolf Nonnenmacher and Ingrid Ertel for their excellent preparation of the figures.

References

1. Davies F, Coles GA, Harper PS, Williams AJ, Evans C, Cochlin D: Polycystic kidney disease re-evaluated: A population-based study. *Q J Med* 79: 477–485, 1991
2. Higashihara E, Nutahara K, Kojima M, Tamakoshi A, Yoshiyuki O, Sakai H, Kurokawa K: Prevalence and renal prognosis of diagnosed autosomal dominant polycystic kidney disease in Japan. *Nephron* 80: 421–427, 1998
3. Lowrie EG, Hampers CL: The success of Medicare's end-stage renal-disease program. *N Engl J Med* 305: 434–438, 1981
4. Anonymous: Incidence and causes of treated ESRD. *Am J Kidney Dis* 18[Suppl 2]: 30–37, 1991
5. Torra R, Darnell A, Cleries M, Botey A, Revert L, Vela E: Polycystic kidney disease patients on renal replacement therapy: Data from the Catalan renal registry. *Contrib Nephrol* 115: 177–181, 1995
6. European dialysis and transplant association registry: Demography of dialysis and transplantation in Europe, 1984. *Nephrol Dial Transplant* 1: 1–8, 1986
7. Anonymous: Incidence and prevalence of ESRD. *Am J Kidney Dis* 32[Suppl 1]: S38–S49, 1998
8. European Polycystic Kidney Disease Consortium: The polycystic kidney disease 1 gene encodes a 14 kb transcript and lies within a duplicated region on chromosome 16. *Cell* 77: 881–894, 1994
9. Mochizuki T, Wu G, Hayashi T, Xenophontos SL, Veldhuisen B, Saris JJ, Reynolds DM, Cai Y, Gabow PA, Pierides A, Kimberling WJ, Breuning MH, Deltas CC, Peters DJM, Somlo S: *PKD2*, a gene for polycystic kidney disease that encodes an integral membrane protein. *Science* 272: 1339–1342, 1996
10. Peters DJM, Sandkuijl LA: Genetic heterogeneity of polycystic kidney disease in Europe. *Contrib Nephrol* 97: 128–139, 1992
11. Roscoe JM, Brissenden JE, Williams EA, Chery AL, Silverman M: Autosomal dominant polycystic kidney disease in Toronto. *Kidney Int* 44: 1101–1108, 1993
12. Wright AF, Teague PW, Pound SE, Pignatelli PM, Macnicol AM, Carothers AD, de Mey RJ, Allan PL, Watson ML: A study of genetic linkage heterogeneity in 35 adult-onset polycystic kidney disease families. *Hum Genet* 90: 569–571, 1993
13. Torra R, Badenas C, Darnell A, Nicolau C, Volpini V, Revert L, Estivill X: Linkage, clinical features, and prognosis of autosomal dominant polycystic kidney disease types 1 and 2. *J Am Soc Nephrol* 7: 2142–2151, 1996

14. Bogdanova N, Dworniczak B, Dragova D, Todorov V, Dimitrakov D, Kalinov K, Hallmayer J, Horst J, Kalaydjieva L: Genetic heterogeneity of polycystic kidney disease in Bulgaria. *Hum Genet* 95: 645–650, 1995
15. Daoust MC, Reynolds DM, Bichet DG, Somlo S: Evidence for a third genetic locus for autosomal dominant polycystic kidney disease. *Genomics* 25: 733–736, 1995
16. de Almeida S, de Almeida E, Peters D, Pinto JR, Távora I, Lavinha J, Breuning M, Prata MM: Autosomal dominant polycystic kidney disease: Evidence for the existence of a third locus in a Portuguese family. *Hum Genet* 96: 83–88, 1995
17. Turco AE, Clementi M, Rossetti S, Tenconi R, Pignatti PF: An Italian family with autosomal dominant polycystic kidney disease unlinked to either the *PKD1* or *PKD2* gene. *Am J Kidney Dis* 28: 759–761, 1996
18. Parfrey PS, Bear JC, Morgan J, Cramer BC, McManamon PJ, Gault MH, Churchill DN, Singh M, Hewitt R, Somlo S, Reeders ST: The diagnosis and prognosis of autosomal dominant polycystic kidney disease. *N Engl J Med* 323: 1085–1090, 1990
19. Gabow PA, Johnson AM, Kaehny WD, Kimberling WJ, Lezotte DC, Duley IT, Jones RH: Factors affecting the progression of renal disease in autosomal-dominant polycystic kidney disease. *Kidney Int* 41: 1311–1319, 1992
20. Ravine D, Walker RG, Gibson RN, Forrest SM, Richards RI, Friend K, Sheffield LJ, Kincaid-Smith P, Danks DM: Phenotype and genotype heterogeneity in autosomal dominant polycystic kidney disease. *Lancet* 340: 1330–1333, 1992
21. Coto E, Sanz de Castro S, Aguado S, Alvarez J, Arias M, Menéndez MJ, Lopez-Larrea C: DNA microsatellite analysis of families with autosomal dominant polycystic kidney disease types 1 and 2: Evaluation of clinical heterogeneity between both forms of the disease. *J Med Genet* 32: 442–445, 1995
22. Hateboer N, van Dijk MA, Bogdanova N, Coto E, Saggat-Malik AK, San Millan JL, Torra R, Breuning M, Ravine D: Comparison of phenotypes of polycystic kidney disease types 1 and 2. *Lancet* 353: 103–107, 1999
23. Lu W, Peissel B, Babakhanlou H, Pavlova A, Geng L, Fan X, Larson C, Brent G, Zhou J: Perinatal lethality with kidney and pancreas defects in mice with a targeted *Pkd1* mutation. *Nat Genet* 17: 179–181, 1997
24. Kim K, Drummond I, Ibraghimov-Beskrovnaya O, Klinger K, Arnaout MA: Polycystin 1 is required for the structural integrity of blood vessels. *Proc Natl Acad Sci USA* 97: 1731–1736, 2000
25. Boulter C, Mulroy S, Webb S, Fleming S, Brindle K, Sandford R: Cardiovascular, skeletal, and renal defects in mice with a targeted disruption of the *Pkd1* gene. *Proc Natl Acad Sci USA* 98: 12174–12179, 2001
26. Wu G, D'Agati V, Cai Y, Markowitz G, Park JH, Reynolds DM, Maeda Y, Le TC, Hou H Jr, Kucherlapati R, Edelmann W, Somlo S: Somatic inactivation of *Pkd2* results in polycystic kidney disease. *Cell* 93: 177–188, 1998
27. Wu G, Markowitz GS, Li L, D'Agati VD, Factor SM, Geng L, Tibara S, Tuchman J, Cai Y, Park JH, van Adelsberg J, Hou H Jr, Kucherlapati R, Edelmann W, Somlo S: Cardiac defects and renal failure in mice with targeted mutations in *Pkd2*. *Nat Genet* 24: 75–78, 2000
28. Pei Y: A “two-hit” model of cystogenesis in autosomal dominant polycystic kidney disease. *Trends Mol Med* 7: 151–156, 2001
29. Markowitz GS, Cai Y, Li L, Wu G, Ward LC, Somlo S, D'Agati VD: Polycystin-2 expression is developmentally regulated. *Am J Physiol* 277: F17–F25, 1999
30. Obermüller N, Gallagher AR, Cai Y, Gassler N, Gretz N, Somlo S, Witzgall R: The rat *Pkd2* protein assumes distinct subcellular distributions in different organs. *Am J Physiol* 277: F914–F925, 1999
31. Ong ACM, Ward CJ, Butler RJ, Biddolph S, Bowker C, Torra R, Pei Y, Harris PC: Coordinate expression of the autosomal dominant polycystic kidney disease proteins, polycystin-2 and polycystin-1, in normal and cystic tissue. *Am J Pathol* 154: 1721–1729, 1999
32. Foggensteiner L, Bevan AP, Thomas R, Coleman N, Boulter C, Bradley J, Ibraghimov-Beskrovnaya O, Klinger K, Sandford R: Cellular and subcellular distribution of polycystin-2, the protein product of the *PKD2* gene. *J Am Soc Nephrol* 11: 814–827, 2000
33. Cai Y, Maeda Y, Cedzich A, Torres VE, Wu G, Hayashi T, Mochizuki T, Park JH, Witzgall R, Somlo S: Identification and characterization of polycystin-2, the *PKD2* gene product. *J Biol Chem* 274: 28557–28565, 1999
34. Gallagher AR, Cedzich A, Gretz N, Somlo S, Witzgall R: The polycystic kidney disease protein *PKD2* interacts with Hax-1, a protein associated with the actin cytoskeleton. *Proc Natl Acad Sci USA* 97: 4017–4022, 2000
35. Koulen P, Cai Y, Geng L, Maeda Y, Nishimura S, Witzgall R, Ehrlich BE, Somlo S: Polycystin-2 is an intracellular calcium release channel. *Nat Cell Biol* 4, 2002
36. Cowley BD Jr, Gudapaty S, Kraybill AL, Barash BD, Harding MA, Calvet JP, Gattone VH II: Autosomal-dominant polycystic kidney disease in the rat. *Kidney Int* 43: 522–534, 1993
37. Schäfer K, Gretz N, Bader M, Oberbäumer I, Eckardt K-U, Kriz W, Bachmann S: Characterization of the Han:SPRD rat model for hereditary polycystic kidney disease. *Kidney Int* 46: 134–152, 1994
38. Obermüller N, Gretz N, Kriz W, van der Woude FJ, Reilly RF, Murer H, Biber J, Witzgall R: Differentiation and cell polarity during renal cyst formation in the Han:SPRD (*cy/+*) rat, a model for ADPKD. *Am J Physiol* 273: F357–F371, 1997
39. Takahashi H, Ueyama Y, Hibino T, Kuwahara Y, Suzuki S, Hioki K, Tamaoki N: A new mouse model of genetically transmitted polycystic kidney disease. *J Urol* 135: 1280–1283, 1986
40. Takahashi H, Calvet JP, Dittmore-Hoover D, Yoshida K, Grantham JJ, Gattone VH: A hereditary model of slowly progressive polycystic kidney disease in the mouse. *J Am Soc Nephrol* 1: 980–989, 1991
41. Obermüller N, Kränzlin B, Verma R, Gretz N, Kriz W, Witzgall R: Renal osmotic stress-induced cotransporter: Expression in the newborn, adult and post-ischemic rat kidney. *Kidney Int* 52: 1584–1592, 1997
42. Appenroth D, Gambaryan S, Winnefeld K, Leiterer M, Fleck C, Bräunlich H: Functional and morphological aspects of thallium-induced nephrotoxicity in rats. *Toxicology* 96: 203–215, 1995
43. Venkatachalam MA, Bernard DB, Donohoe JF, Levinsky NG: Ischemic damage and repair in the rat proximal tubule: Differences among the S₁, S₂, and S₃ segments. *Kidney Int* 14: 31–49, 1978
44. Witzgall R, Brown D, Schwarz C, Bonventre JV: Localization of proliferating cell nuclear antigen, vimentin, c-Fos, and clusterin in the post-ischemic kidney. Evidence for a heterogeneous genetic response among nephron segments, and a large pool of mitotically active and dedifferentiated cells. *J Clin Invest* 93: 2175–2188, 1994
45. Witzgall R: The proximal tubule phenotype and its disruption in acute renal failure and polycystic kidney disease. *Exp Nephrol* 7: 15–19, 1999

46. Safirstein R, Price PM, Saggi SJ, Harris RC: Changes in gene expression after temporary renal ischemia. *Kidney Int* 37: 1515–1521, 1990
47. Nouwen EJ, Verstrepen WA, Buysens N, Zhu M-Q, de Broe ME: Hyperplasia, hypertrophy, and phenotypic alterations in the distal nephron after acute proximal tubular injury in the rat. *Lab Invest* 70: 479–493, 1994
48. Bergeron M, Thiéry G: Three-dimensional characteristics of the endoplasmic reticulum of rat renal tubule cells, an electron microscopy study in thick-sections. *Biol Cell* 42: 43–48, 1981
49. Bergeron M, Gaffiero P, Thiéry G: Segmental variations in the organization of the endoplasmic reticulum of the rat nephron. A stereomicroscopic study. *Cell Tissue Res* 247: 215–225, 1987